AD-A032 716 NAVAL ACADEMY ANNAPOLIS MD F/G 1/2

INVESTIGATION INTO THE FEASIBILITY OF UTILIZING WIND SHEAR FOR --ETC(U)

JUN 76 F G JOHNSON

UNCLASSIFIED USNA-TSPR-78 NL

1 OF 1

AD A032716

END

DATE FILMED

1-77

(23)

A TRIDENT SCHOLAR PROJECT REPORT

NO. 78

INVESTIGATION INTO THE FEASIBILITY OF UTILIZING WIND SHEAR FOR OBTAINING CONTINUOUS NON-POWERED FLIGHT

UNITED STATES NAVAL ACADEMY
ANNAPOLIS, MARYLAND
1976

United States Naval Academy - Trident Scholar project report, no. 78.(1976)

6 INVESTIGATION INTO THE FEASIBILITY OF UTILIZING WIND SHEAR FOR OBTAINING CONTINUOUS NON-POWERED FLIGHT.

9 Research rept.,

21 Report on A Trident Scholar Project Report

by

10

Midshipman Frederick G. Johnson, Class of 1976

U. S. Naval Academy

Annapolis, Maryland

14 USNA-TSPR-78

Associate Professor Vadim V. Utgoff

Aerospace Engineering Department

Accepted for Trident Scholar Committee

Chairman

11 3 June 1976

Date

12 56p.

245 600
bpf

ABSTRACT

The feasibility of utilizing an atmospheric velocity gradient for obtaining continuous non-powered flight was analyzed mathematically and experimentally. It was discovered that there seems to be no theoretical bar to using wind shear for this purpose. The velocity gradients in the upper atmosphere were found to be too weak for maintaining continuous non-powered flight, but in the vicinity of the earth's boundary layer wind shear strengths necessary for this purpose were observed.

A theoretical flight pattern was developed, numerically analyzed and flight tested using a powered aircraft to simulate high performance sailplanes. Though an increase in aircraft performance was realized a zero net loss of altitude was not achieved. It is concluded, however, that further research is warranted, especially concerning the related topics of jet stream shears, vertical updraft considerations and more efficient flight schedules.

ACKNOWLEDGEMENTS

The research reported herein was funded by the Naval Academy Research Council and the Naval Air Systems Command, Department of the Navy.

Special thanks is also extended to Associate Professor Vadym V. Utgoff whose keen understanding of the dynamic soaring problem and superior piloting ability were the cornerstones of this project. His patience, guidance and continuous encouragement were of immeasurable value to the author.

TABLE OF CONTENTS

INTRODUCTION

Numerous articles have been written dealing with the meteorological phenomenon known as wind shear. Wind shear is a velocity gradient with increasing altitude; a wind profile which must exist in order to account for the difference between relatively large upper atmosphere winds and the air at the earth's surface which is essentially at rest.

Such a wind differential has become an important design consideration of modern skyscrapers. Structural allowances must be made for the increased wind loading experienced by tall buildings.[1] Recently studies concerning the effects of velocity gradients upon landing aircraft have been undertaken. The National Aeronautics and Space Administration sponsored an investigation into such effects.[2] Analytic studies utilizing a digital computer simulation show that wind shear produces a significant deviation in the touchdown point of a landing aircraft as compared to the same aircraft landing under exactly the same conditions except for the absence of shear.[3] Additionally, the National Transportation Safety Board acknowledged wind shear as a primary contributor to the crash of an Iberia airliner on December 17, 1973.[4] Therefore the existence of velocity gradients has emerged in recent years as an

important engineering consideration.

Types Of Wind Shear

Evidence suggests that there exist two characteristic types of wind shear. The first is found near the earth's surface and closely resembles the shape of a typical viscous flow boundary layer. Beyond the well defined boundary layer, however, is a more subtle, gradually increasing velocity gradient. This gradient has been referred to as upper level shear.

Boundary Layer Shear

A great deal of research has been done on the subject of the earth's boundary layer shear. This is probably due to the previously mentioned importance of boundary layer shear in recent engineering considerations and its relative ease of measurement due to its close proximity to the ground.

Boundary layer shear is a relatively common occurrence because of its dependance upon surface friction effects rather than prevailing weather conditions. The single major exception to this generalization is pointed out by Mr. Davenport in his initial study of boundary layer shear. He found that in severe thunderstorms or squalls the boundary layer breaks down. Under such violent frontal conditions the atmosphere directly above the earth is highly turbulent and unstable, the result being that a distinct, gradient style increase in velocity with altitude is greatly reduced.[5]

The boundary layer may usually be expected to be somewhat turbulent. Obstructions such as buildings, hills and trees give rise to gyrating vorticies and vertical thermal currents further add to the instability of the boundary layer.

Various formulas have been suggested to describe the wind profile in the boundary layer but the most popular is the power equation;

$$V(z) = kz^{1/a}$$

where V(z) is the wind velocity at altitude z, k is a strength coefficient which must be determined expirementally, and a is dependant upon the terrain (i.e. surface roughness). Based upon extensive worldwide research Mr. Davenport offers the following guidelines for assigning a value to a;[6]

1. open country, flat lands, grassland, large bodies of water and tundra; a=7
2. wooded countryside, rough coastal belt, outskirts of a city; a=3.5
3. center of a large city; a=2.5

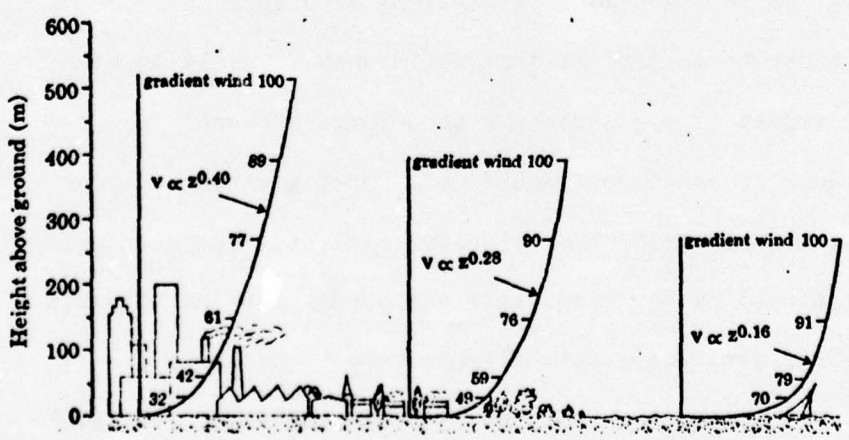

Figure 1. Wind profiles described by Davenport's power equation parameters over various terrain.

Upper Level Shear

Analytic research concerning upper level shear has been much less extensive than for boundary layer shear. High altitude shear requires much more sophisticated measuring systems and is of less direct engineering importance due to its relative weakness and its distance from the earth's surface.

Actual meteorological data confirms the existence of upper level wind shear. Figure 2 displays a velocity gradient which occurred over Omaha in January, 1974. The strength of the gradient was .0065 ft/sec•ft.[7] Two important characteristics may be noted about the non-boundary layer shear described in Figure 2. First, as mentioned previously, the gradient is quite weak, increasing only .65 ft/sec in every 100 feet. This fact alone suggests that detection and accurate measurement of upper level shear would demand painstaking care. Secondly, the velocity gradient above the boundary layer may reasonably be represented by a straight line function.

In order to achieve maximum efficiency from flying time for this report it was necessary to determine exactly what type of weather conditions would prove most advantageous for detecting and measuring the velocity gradient. In particular, a forecast outline for wind shear was needed for the Virginia and Maryland area where data flights were to be made.

Mr. W. Bonner discussed the characteristics of low level wind maxima in an article written for Monthly Weather Review.

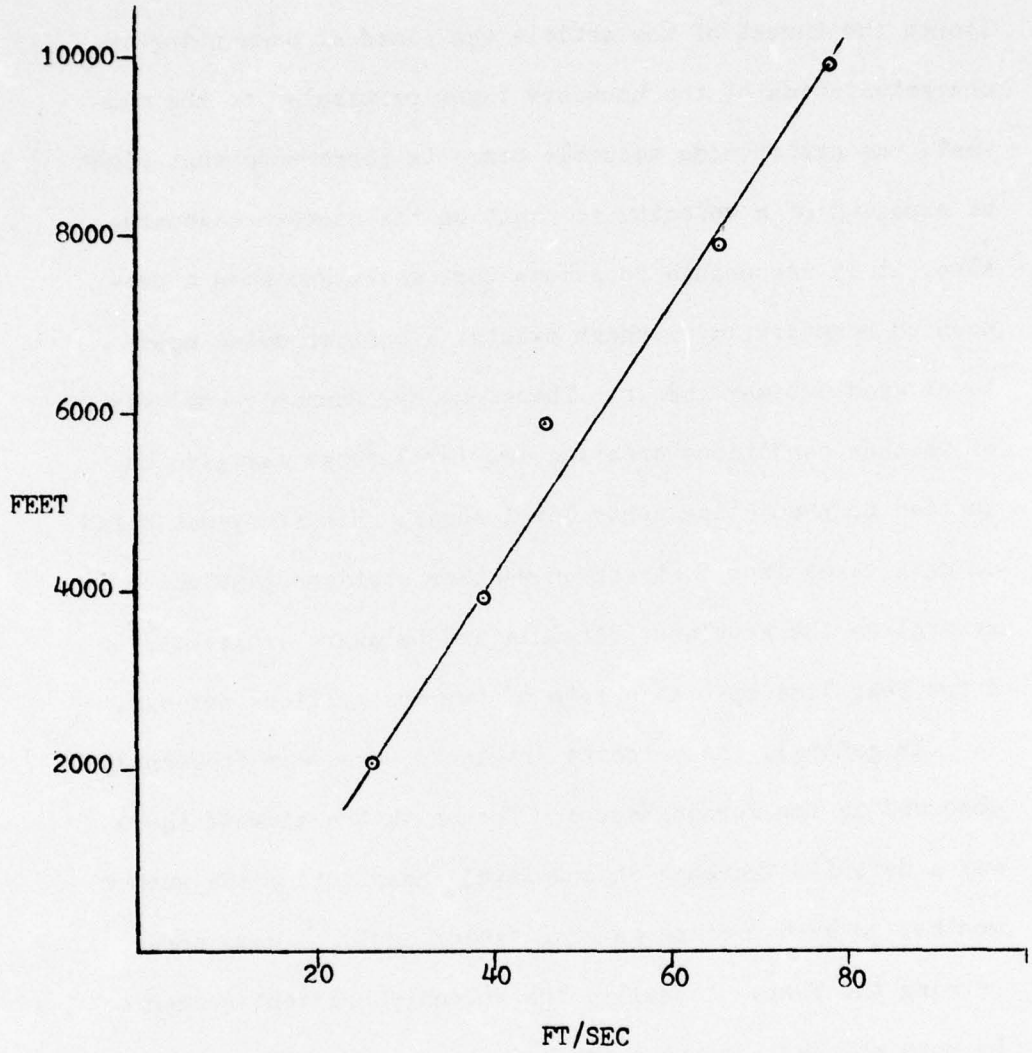

FIGURE 2

WIND VELOCITY vs ALTITUDE

Omaha, Nebraska
1200 7 January 1974
Shear = .0065 (FT/SEC)/FT

Though the thrust of the article was aimed at commenting on characteristics of the boundary layer particular to the mid-west, the author made valuable comments concerning what might be expected of a velocity gradient on the Eastern seaboard. Also, it is reasonable to assume that where and when a pronounced boundary layer shear exists, a corresponding upper level gradient may appear. Therefore Mr. Bonner's analysis of weather conditions creating low level shear may also be applied to predicting upper level shear. His study was based on data taken from forty-seven weather stations (including several in the Maryland, Virginia and Delaware areas) during a two year time span at a rate of two observations per day.

In general, the velocity gradients were more frequently observed in the morning hours. Though in the midwest there was a definite increase in low level shear during the summer months, no such precise generalization could be made concerning the East. Actually, the velocity gradient seemed to be more abundant in the Annapolis area between the months of October and March. In addition, such a velocity gradient was usually from the north or northwest.[8]

An independant U. S. Army Missile Command report supports Mr. Bonner's observations. It shows an increase in the strength of the shear in the vicinity of Annapolis's longitude during the fall and winter month s.[9] Figure 3 is a graphical display of some of the results of this report.

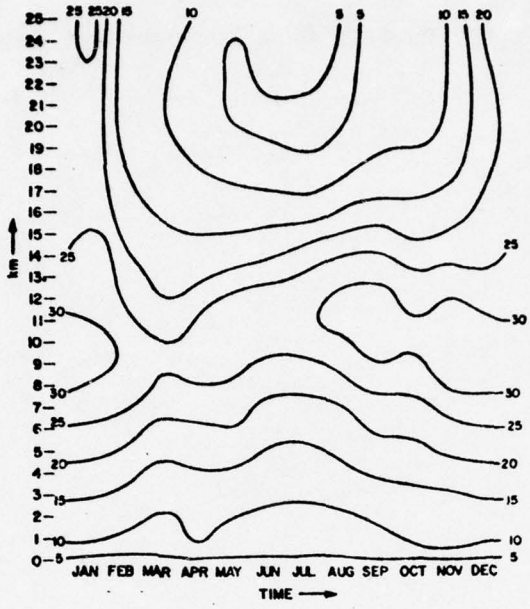

Figure 3. *Time section of wind shear* (m/sec•km) near longitude 80°W. Annapolis longitude is approximately 76°30'W.

Based upon these two reports the following guidelines were devised to govern the choice of days for data collecting flights.

Flights should me made;

a.) during the late fall, winter and possibly early spring months.

b.) over the ocean, similar large body of water or above about one thousand feet to avoid ground induced turbulence and friction effects.

c.) during the morning hours to avoid afternoon convection currents.

d.) on a day with strong northerly surface winds following the passage of a low pressure cold front.

ANALYTIC DISCUSSION

The effect of wind shear upon an aircraft is that of either acceleration or deceleration, depending upon whether the speed in inertial space (ground speed) is increasing or decreasing. Since the shear is a velocity differential with altitude the aircraft must not be moving perpendicular to the wind direction. In crosswind flight no longitudinal acceleration or deceleration due to the wind shear would occur.

Figure 4 shows the aircraft center of gravity descending in a wind shear parallel to the wind direction. The positive directions have been indicated. The flight angle γ has been chosen positive clockwise from the x axis. Summing the forces in the x and y directions:

$$\Sigma F_x = Ma_x = L\sin\gamma - D\cos\gamma \tag{1}$$

$$\Sigma F_y = 0 = L\cos\gamma - W + D\sin\gamma \qquad (D\sin\gamma \approx 0) \tag{2}$$

The wind direction has been assumed to be unidirectional, acting only parallel to the horizontal axis, and the gradient shape represented by a straight line function. Since the wind direction is assumed to act only parallel to the x axis, only inertial acceleration in that direction may exist.

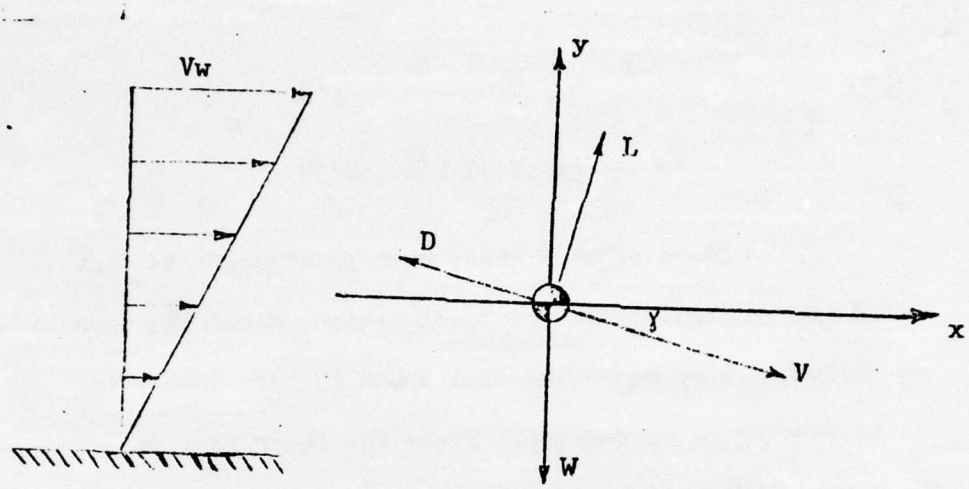

Figure 4. Aircraft center of gravity descending with linear shear.

Small angle approximations may be applied because the descent angle for best glide flight is in general quite small. This is particularly true for high performance sailplanes and even holds true for most general purpose powered aircraft.

Therefore;

$$\cos\gamma=1$$
$$\sin\gamma=\gamma$$
$$\tan\gamma=\gamma$$

where γ is measured in radians.

Equations (1) and (2) may now be simplified;

$$Ma_x=L\gamma-D \tag{3}$$

$$L=W \tag{4}$$

Combining equations (3) and (4) yields

$$Ma_x=W\gamma-D \tag{5}$$

where $D=qS(C_{Dmin}+C_L^2/\pi AR\, e)$ (6)

$$q=\tfrac{1}{2}\rho V^2 \tag{7}$$

Again, the acceleration in the horizontal direction is due to a change in the aircraft's ground speed.

$$a_x=\frac{dVg}{dt} \tag{8}$$

The aircraft's groundspeed is the sum of its true airspeed and the wind speed;

$$Vg=V+Vw \tag{9}$$

Here it may be noted that again the small angle approximation $\cos\gamma$ has been applied so that $V=V\cos\gamma$. If the velocity is held constant then the acceleration becomes

$$a_x=\frac{dVw}{dt} \tag{10}$$

The change in wind speed, however, may be considered the product of the rate of descent and the velocity gradient;

$$\frac{dVw}{dt}=-\frac{dVw}{dh}\cdot\frac{dh}{dt} \tag{11}$$

This product is negative ($dh/dt<0$) indicating that the acceleration is in fact a deceleration; the airplane is losing ground speed while maintaining a constant airspeed.

Equation (11) may be further rewritten realizing that the rate of descent dh/dt is also the downward velocity $Vy=V\sin\gamma$.

$$\frac{dVw}{dt} = \frac{-dVw}{dh} \cdot Vy = \frac{-dVw}{dh} \cdot V\gamma \tag{12}$$

Combining equations (5), (6) and (12) yields

$$\frac{-WV\gamma dVw}{g\ dh} = W\gamma - qSC_{Dmin} - qC_L{}^2S/\pi AR\ e \tag{13}$$

but $C_L{}^2 = (L/qS)^2 = (W/qS)^2$ (14)

so equation (13) becomes

$$\frac{-WV\gamma dVw}{g\ dh} = W\gamma - qSC_{Dmin} - W^2/qS\pi AR\ e \tag{15}$$

Dividing through by W/g and rearranging terms;

$$\frac{-V\gamma dVw}{dh} - g\gamma = -g\left(\frac{qSC_{Dmin}}{W} + \frac{W}{qS\pi AR\ e}\right) \tag{16}$$

Solving for the angle of descent;

$$\gamma = \frac{g}{\left(g + \frac{VdVw}{dh}\right)}\left(\frac{qSC_{Dmin}}{W} + \frac{W}{qS\pi AR\ e}\right) \tag{17}$$

With no velocity gradient present (dVw/dh=0 or cross-wind flight);

$$\gamma = \frac{qSC_{Dmin}}{W} + \frac{W}{qS\pi AR\ e} = \frac{D}{L} \tag{18}$$

Equations (17) and (18) show that a constant velocity descent with a wind shear differs from a descent without a shear (or crosswind to a shear) by a factor F;

$$F = \frac{g}{\left(g + \frac{VdVw}{dh}\right)} \tag{19}$$

Taking as an example the shear of Figure 2 of the Introduction, with a velocity of 100 mph = 146.67 ft/sec, F = .97. Thus a flight angle is reduced three percent in a wind shear of .0065 ft/sec/ft at 100 mph. Using a stronger

shear of .02 results in F = .92, an eight percent reduction of the flight angle. A reduction of flight angle (increase in F) may also apparently result from an increase in true airspeed V. However, it must be remembered that this analysis has at its foundation the small angle approximations which may be violated at higher airspeeds in the descent.

Equation (16) provides a theoretical method for measuring a straight line wind shear;

$$\frac{dVw}{dh} = \frac{g}{R/D}\left(\frac{qSC_{Dmin}}{W} + \frac{W}{qS\pi AR\,e} - \frac{R/D}{V}\right) \tag{20}$$

where R/D is the rate of descent at constant velocity V.

$$R/D = \frac{h_2 - h_1}{t_2 - t_1}$$

Since q depends upon temperature and the aircraft weight will vary due to the loss of fuel (powered aircraft assumed) an average of those two quantities must be determined for a given descent. An overly long descent might cause errors due to inaccurate temperature or weight averages being applied to equation (20).

Though the foregoing analysis demonstrates the theoretical effect of wind shear upon an aircraft, it is of little practical value. Glide angle reduction in a constant velocity descent is quite small. To reach a significant reduction (i.e. 50% or better) an extremely large

shear would be required. Shears of that order of magnitude have not been observed in nature. Also, though a similar interpretation of a constant velocity climb into the wind yields a result equivalent to the descent, it is obvious that a constant velocity climb is not practical for any non-powered aircraft. Another problem with this analysis is that it does not allow for a convenient interpretation of the transition from the descent to the climb. Some type of realistic climb and descent schedule must be devised which can be followed by the pilot without excessive difficulty.

Consider a purely circular flight path. Figure 5 shows the aircraft's movement as projected onto the ground. Flight path heading is measured clockwise from the wind direction to the aircraft velocity vector.

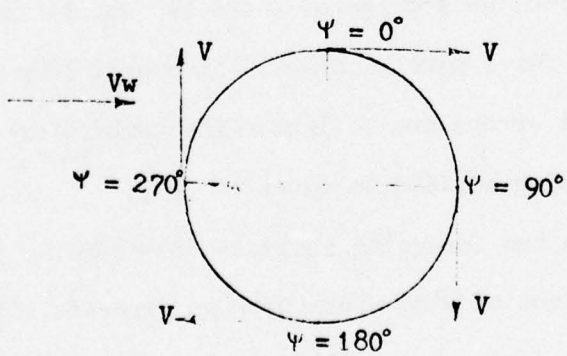

Figure 5. Circular flight path viewed from above.

The aircraft's groundspeed is the sum of its true airspeed and the component of wind acting along the flight path;

$$Vg = V + Vw\cos\Psi \tag{21}$$

The inertial acceleration experienced by the aircraft due to climbing and descending through the shear is again the change in groundspeed.

$$a_x = \frac{dVg}{dt} = \frac{dV}{dt} - Vw\sin\Psi\frac{d\Psi}{dt} + \cos\Psi\frac{dVw}{dt} \tag{22}$$

where the x direction is now taken to correspond to the direction of the flight path.

For this discussion the velocity of the aircraft is limited to a sinusoidal variation so over one period of the flight cycle its derivative may be assumed zero.

Altitude, true airspeed and climb angle may be written as functions of the flight angle. The climb angle will be zero at $\Psi = 270°$ and $90°$. It will reach a maximum positive value at $\Psi = 180°$ and a minumum at $\Psi = 0°$. Velocity and altitude will oscillate about median values $\overline{V}$ and $\overline{h}$ respectively in a sinusoidal manner. Airspeed reaches a maximum at $\Psi = 90°$, while the aircraft is at the highest point in the cycle at $\Psi = 270°$. These quantities may be converted to the time domain by assuming a constant turning rate Ω.

$$\Psi = \Omega t \tag{23a}$$

$$d\Psi = \Omega dt \tag{23b}$$

The equations for altitude, velocity and glide angle are;

$$h = \bar{h} - \tfrac{1}{2}\Delta h \sin\Psi \tag{24}$$

$$V = \bar{V} + \tfrac{1}{2}\Delta V \sin\Psi \tag{25}$$

$$\gamma = -\gamma_{max}\cos \tag{26}$$

where

$$\bar{V} = (V_{max} + V_{min})/2$$

$$\Delta V = (V_{max} - V_{min})$$

$$\Delta h = (h_{max} - h_{min})$$

Returning now to equation (22), substituting in equation (11) for the rate of change of the wind velocity and multiplying by the aircraft mass produces the inertial force due to the wind shear acting on the aircraft;

$$F = \frac{W}{g}\left(\cos\Psi \frac{dVw}{dh}\frac{dh}{dt} - Vw\sin\Psi\frac{d\Psi}{dt}\right) \tag{27}$$

The term F in this equation should not be confused with the factor determined in equation (19). When this force is less than zero, the airplane is decelerating in inertial space. This occurs during the climb when the flight heading is between 90° and 270°. During this interval the aircraft is extracting energy from the wind. Similarly in the descent the aircraft is accelerating relative to the ground and it must give up energy by either losing altitude or by providing thrust from an engine.

The power available to the aircraft due to the wind shear is;

$$Pa = -FV = -\frac{VW}{g}\left(\cos\Psi\frac{dVw}{dh}\frac{dh}{dt} - Vw\sin\Psi\Omega\right) \tag{28}$$

Negative power represents power supplied by the wind shear. Equation (23b) has been substituted into equation (28) to replace the time rate of change of the aircraft flight heading.

The climb or descent rate (dh/dt) must now be analyzed in terms of the flight heading. Assuming the exchange of energy during a climb or descent may be represented by a loss-gain relationship between kinetic and potential energy;

$$\Delta PE = \Delta KE$$

$$mg\Delta h = \tfrac{1}{2}m\Delta V^2$$

$$\Delta h = \Delta V^2/2g = (V_{max}^2 - V_{min}^2)/2g \tag{29}$$

also, the climb rate will vary throughout the cycle, so;

$$dh/dt = -(dh/dt)_M \cos\Psi \tag{30}$$

The subscript M indicates maximum climb rate. Using equation (23b) and integrating over the climb half of the period;

$$\Delta h = \int_{90^\circ}^{270^\circ} dh = \frac{-(dh/dt)_M}{\Omega}\int_{90^\circ}^{270^\circ}\cos\Psi d\Psi$$

$$\Delta h = \frac{2(dh/dt)_M}{\Omega} \tag{31}$$

Equations (29) and (31) may be combined to discover the maximum rate of climb;

$$(dh/dt)_M = \Omega \Delta V^2/4g \tag{32}$$

Now with the exception of the wind speed the power available may be written in terms of the flight heading by substituting equations (25), (30) and (32) into equation (28);

$$Pa = \frac{W\Omega}{g}(\overline{V} + \tfrac{1}{2}\Delta V\sin\Psi)(\cos^2\Psi \frac{dVw}{dh}\frac{\Delta V^2}{4g} + Vw\sin\Psi) \tag{33}$$

The wind speed and its derivative are also functions of the flight heading and vary in a sinusoidal manner as the aircraft traverses the flight path.

Both boundary layer shear and upper level shear may be represented by the same power equation;

$$Vw = kh^{1/a} = k(\overline{h} + \tfrac{1}{2}\Delta h\sin\ )^{1/a} \tag{34a}$$

$$dVw/dh = \frac{k}{a}\, h^{1/a-1} = \frac{k}{a}(\overline{h} + \tfrac{1}{2}\Delta h\sin\ )^{1/a-1} \tag{34b}$$

For boundary layer shear the Davenport parameters discussed previously may be applied while if a linear shear is experienced a = 1 and k is the slope of the shear.

Now an equation for power available may be written completely in terms of the flight heading.

$$Pa = \frac{W\Omega}{g}(\overline{V} + \tfrac{1}{2}\Delta V\sin\Psi)(\cos^2\Psi \frac{k\Delta V^2}{4g} + k(\overline{h} - \tfrac{1}{2}\Delta h\sin\Psi)\sin\Psi) \tag{35}$$

A linear shear of slope k has been assumed for equation (35). Consequently $\overline{h}$ may need adjustment so that the

shear graph intersects the horizontal axis at the origin. (Note the extrapolation of Figure 2 to the velocity axis.) In equation (35) $k = dVw/dh$.

Equations (31) and (32) may now be combined to replace $\frac{1}{2}\Delta h$ in the power equation;

$$Pa = \frac{W\Omega}{g}(\bar{V}+\tfrac{1}{2}\Delta V\sin\Psi)\left(\frac{k\Delta V^2}{4g}\cos^2\Psi + k\bar{h}\sin\Psi - \frac{k\Delta V^2}{4g}\sin^2\Psi\right)$$

but $(\cos^2\Psi - \sin^2\Psi) = \cos 2\Psi$.

Therefore the power equation finally reduces to

$$Pa = \frac{W\Omega}{g}(\bar{V} + \tfrac{1}{2}\Delta V\sin\Psi)\left(\frac{k\Delta V^2\cos 2\Psi}{4g} + k\bar{h}\sin\Psi\right) \qquad (36)$$

At this point it is desireable to determine the energy provided to the aircraft due to the wind shear in one cycle and compare with the energy required (drag effects) during the course of the same cycle. The two resulting energy expressions may be equated to determine the parameters necessary to prevent a loss of altitude in the cycle.

The energy available to the aircraft due to the wind shear over one cycle is;

$$Ea = \int Pa\, dt = \frac{1}{\Omega}\int_0^{2\pi} Pa\, d\Psi \qquad (37)$$

Integrating equation (36) produces an expression for the energy available;

$$Ea = \frac{W\Delta V\pi}{2g}\left(\frac{\bar{V}^2}{g}k + Vw\right) \qquad (38)$$

The energy required to complete one cycle is the integration of the power required expression of the aircraft.

Flight testing of the circular flight path proved unsatisfactory and impractical even under simulated high glide ratio conditions (see Appendix 1). The following observed conditions contributed to the inadequacy of the circular approach to the dynamic soaring problem.

The flight schedule demanded far too much effort from the pilot in order to conform exactly to the theoretical model. Coordination of flight heading, velocity and altitude proved to be a formidable task. It was virtually impossible to obtain the exact sinusoidal variations of the flight parameters as required by theory. The result was that a truly constant turning rate was not achieved; bank angle varied from a spectacular nearly vertical wing-over at the high altitude point and a medium banked turn at the low altitude end. Also, as may be ascertained from Figure 5, the aircraft was not taking maximum advantage of the wind shear effect through most of the cycle. The component of wind acting along the longitudinal axis of the aircraft varies sinusoidally. Thus the flight path obviously reduces the effect of the wind shear upon the flight angle in the ascent or descent phases

of the flight schedule.

From these unsatisfactory characteristics arose the desire to modify the circular flight path by making the ascent and descent legs entirely parallel to the wind direction. Figure 6 depicts such a flight schedule and shall be hereafter referred to as the "racetrack" flight path.

The racetrack flight schedule may be broken into three portions for examination. The first is the combination of the ascent and descent legs, the second is the high speed turn at the low altitude end and the third is the low speed turn at the high altitude end.

In order to maximize efficiency of the aircraft's exchange of potential and kinetic energy in the climb and descent, the phugoid oscillation mode of the aircraft will be utilized. The phugoid oscillation is a stick-fixed, long period, lightly damped natural longitudinal oscillitory mode in which the aircraft alternately exchanges airspeed for altitude at a natural frequency. A detailed mathematical evaluation and discussion of the phugoid oscillation is contained in Etkin's Dynamics of Flight or other similar stability and control texts.

The velocity of the aircraft in the ascent and descent legs is described by the relation

$$V = \bar{V} + \Delta V/2 \cos wt \tag{39}$$

$$w = 2\pi f \tag{40}$$

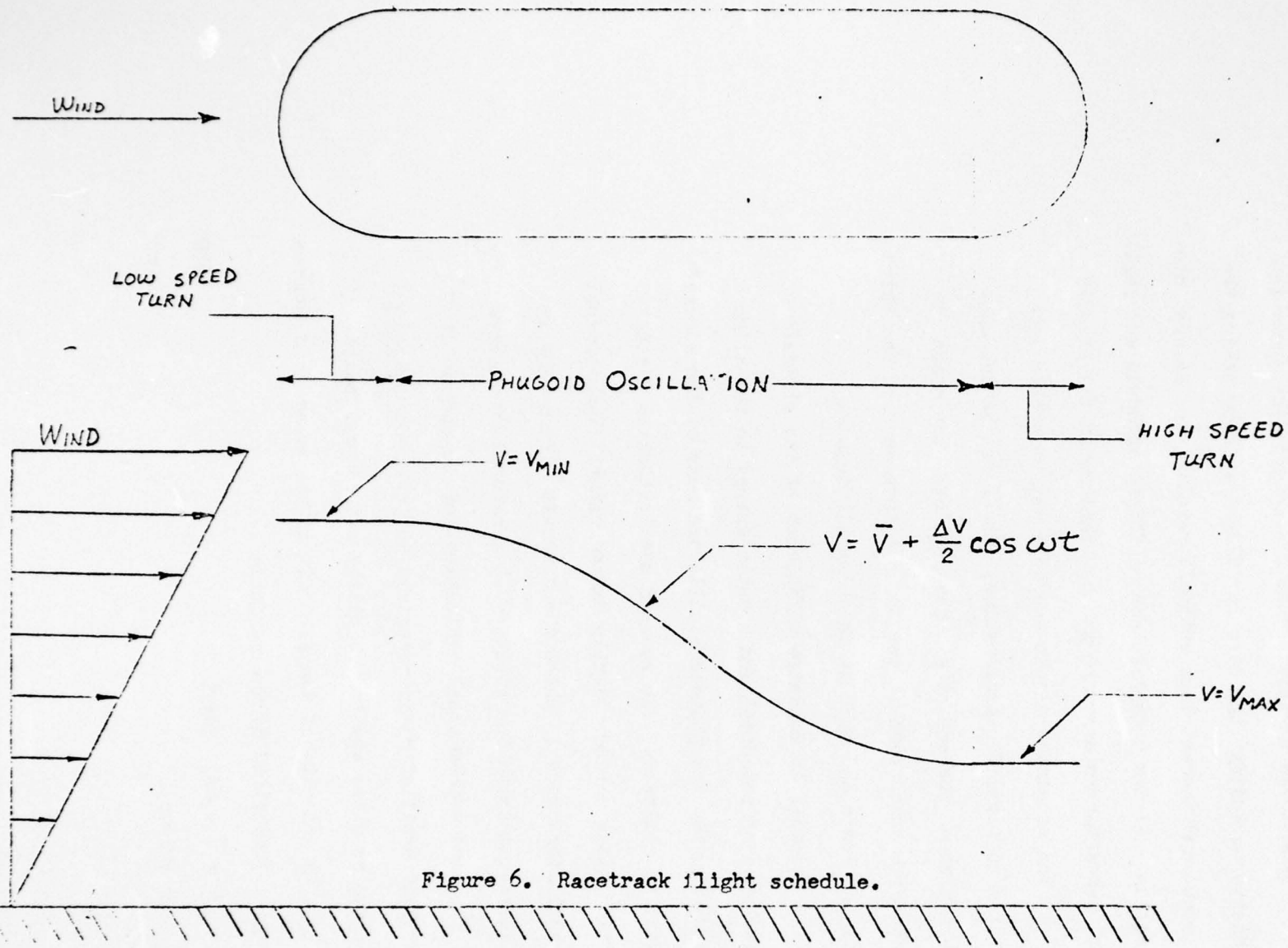

Figure 6. Racetrack flight schedule.

$\overline{V}$ and ΔV possess the same definitions as in the circular case, w is the phugoid angular frequency and f is the phugoid frequency in cycles per second.

The sign of the cosine term in equation (39) depends upon where zero time is established. If zero time is considered to be at the high altitude low speed end the sign is negative. Conversely if t=0 at the high speed end the sign is positive.

At each end of the phugoid oscillation a turn at constant altitude and velocity is assumed. Each turn must be tailored for minimum energy expenditure while they must also necessarily be limited by phugoid maximum and minimum velocities, structural limitations (as determined by the manufacturer's recommended maximum load factor), and pilot physiological response to turn loading.

The advantages of this flight path as opposed to the circular path are readily discerned. The ascent and descent legs are performed entirely parallel to the wind direction and therefore make maximum use of the longitudinal wind shear effect. Also, this schedule makes it easier for the pilot to conform to theory.

Piloting procedure is merely to;

1. Create the phugoid oscillation with the desired velocity parameters,

2. Provide a "tap" to the stick in the descent to counteract the natural phugoid damping and maintain velocity parameters,

3. At each extreme altitude point in the flight schedule complete a constant velocity turn of 180 degrees and release the stick so that the aircraft may resume its oscillation.

The power required for the aircraft to complete one cycle of the racetrack flight schedule is the sum of the power required in both turns and the power required for one complete phugoid oscillation.

The power required for a level turn is;

$$Pr = \Gamma V^3 \left(C_{Dmin} + \frac{n^2 W^2}{\Gamma^2 \Lambda V^4}\right) \tag{41}$$

For convenience the constants $\frac{1}{2}\rho S$ and $\pi AR e$ have been replaced with Γ and Λ respectively.

The minimum drag coefficient is found by taking the derivative of the power with respect to velocity and setting the resulting expression equal to zero. Solving for C_{Dmin} yields;

$$C_{Dmin} = \frac{1}{3}\left(\frac{W^2}{\Gamma^2 V_o^4 \Lambda}\right) \tag{42}$$

where V_o is the speed for minimum sink rate (minimum power). The minimum power required for level flight may now be written;

$$P_o = \frac{W^2}{3\Gamma V_o \Lambda} + \frac{W^2}{\Gamma V_o \Lambda} \tag{43}$$

Power required, divided by the aircraft weight produces the sink rate. From equation (43) then the minimum sink rate may be expressed;

$$R/S_o = \frac{4W}{3\Gamma V_o A} \tag{44}$$

Substituting equations (42) and (44) into equation (41) produces a simplified, more useful form of the power required equation;

$$Pr = \frac{W V^3 R/So}{4 V_o^3} + \frac{3 W R/So V_o n^2}{4 V} \tag{45}$$

Of course, the load factor itself is a function of velocity and may be replaced by the following steps;

$$n = \sec \Phi \tag{46a}$$

$$\tan \Phi = V\Omega/g \tag{46b}$$

$$n = \sqrt{(V\Omega/g)^2 + 1} \tag{46c}$$

Now the power required may be written in terms of the turning rate.

$$Pr = \frac{W R/S_o}{4} (V/V_o)^3 + \frac{3 W R/S_o \Omega^2 V_o V}{4 g^2} + \frac{3 W R/S_o V_o}{4 V}$$

The energy required for the turn is;

$$Er = \int_0^{\pi/\Omega} Pr \, dt$$

$$Er = \frac{W\Pi}{\Omega}\left(\frac{R/S_o}{4}(V/V_o)^3 + \frac{3\,R/S_o}{4}(V_o/V)\right)$$

$$+ W\Pi\Omega\,\frac{3\,R/S_o\,V_o\,V}{4\,g^2} \qquad (47)$$

The theoretical turning rate for minimum energy expenditure may be calculated from equation (47) to be

$$\Omega(\text{minimum energy}) = g\sqrt{\frac{(V/V_o)^3 + 3(V_o/V)}{3V_oV}} \qquad (48)$$

This theoretical result, however, produces unacceptably large bank angles and cannot practically be used as a turn criterion. In the numerical analysis which follows this section a bank angle of forty-five degrees will be assumed. Obviously it is easier for the pilot to conform to a constant bank angle than for a specified turning rate.

At the high speed end the pilot may wish to choose any convenient speed less than the aircraft's rated maximum speed. A suggested criteria for V_{max} would be the maneuvering speed, or the speed recommended by the manufacturer for mild aerobatics.

In choosing the minimum velocity for the racetrack schedule the pilot may wish to utilize the following technique: First a desireable bank angle must be chosen and equation (46a) employed to find the load factor corresponding to that bank angle. The stall speed in a turn varies

directly with the square root of the load factor in the turn;

$$V(\text{stall in turn}) = V(\text{stall})\sqrt{n} \tag{49}$$

The load factor in a 45° banked turn is n = 1.4. For the numerical analysis V_{min} will be taken to be the stall speed times the square root of 1.4. Since the turn for a sailplane cannot be truly level, the load factor will actually be slightly smaller and therefore a margin of safety need not be utilized.

Now the power required to complete the phugoid oscillation will be examined. From equation (43) with the load factor equal to one,

$$Pr = \frac{R/S_o\ W}{4}\ (V^3/V_o^3 + 3V_o/V) \tag{50}$$

The velocity for this portion of the flight is given by equation (39). Upon substitution and expansion, equation (50) becomes;

$$Pr = \frac{R/S_o\ W}{4}\left[(\bar{V}/V_o)^3 + \frac{3\bar{V}^2\Delta V}{2V_o^3}\cos wt + \frac{3\bar{V}\Delta V^2}{4V_o^3}\cos^2 wt + \frac{1}{8}(\Delta V/V_o)^3\cos^3 wt + 3V_o(\bar{V} + \tfrac{1}{2}\Delta V\cos wt)^{-1}\right] \tag{51}$$

The energy required is obtained by integrating equation (51) over one phugoid period.

$$Er = \int_0^{2\pi/w} Pr \, dt$$

All odd powers of cosine drop out in the integration. Therefore the result of the integration is;

$$Er = \frac{R/S_o \; W\pi \, \overline{V}}{2 \; w \; V_o^3} \left(\overline{V}^2 + \frac{3}{2}(\Delta V/2)^2 \right) + \frac{3\pi \, R/S_o \; V_o}{2w\sqrt{V_{max} V_{min}}} \qquad (52)$$

The total energy required for the racetrack flight schedule is the sum of equations (47) and (52).

$$Er = \frac{W\pi R/S_o}{4}\left[\frac{1}{\Omega_1}\left((V_{max}/V_o)^3 + 3V_o/V_{max}\right) + \frac{\Omega_1 3\ V_o\ V_{max}}{g^2}\right]$$

$$+ \frac{W\pi R/S_o}{4}\left[\frac{1}{\Omega_2}\left((V_{min}/V_o)^3 + 3V_o/V_{min}\right) + \frac{\Omega_2 3\ V_o\ V_{min}}{g^2}\right]$$

$$+ \frac{W\ R/S_o\pi\bar{V}}{2\ w\ V_o^3}\left(\bar{V}^2 + \frac{3}{2}(\Delta V/2)^2\right) + \frac{3\ R/S_o\ V_o\pi}{2w\sqrt{V_{max}V_{min}}}$$

where $V_{min} = \sqrt{1.4}\ V(\text{stall})$

$\Omega_1 = g/V_{max}$

$\Omega_2 = g/V_{min}$

The power available from the wind is;

$$Pa = m \frac{dVw}{dt} V = W \frac{dVw}{dh} \frac{dh}{dt} V \tag{54}$$

Taking time zero to be at the beginning of the ascent ($V(0) = V_{max}$), the equations for the flight parameters are merely sinusoidal functions of the phugoid frequency.

$$V = \overline{V} + \tfrac{1}{2} \Delta V \cos wt \tag{39}$$

$$\gamma = \gamma_{max} \sin wt \tag{55}$$

$$dh/dt = (dh/dt)_{max} \sin wt \tag{56}$$

Evaluation of $(dh/dt)_{max}$ is similar as for the circular case.

$$\Delta h = \int_0^{\pi/\omega} (dh/dt)_{max} \sin wt \, dt$$

$$\Delta h = -\frac{2}{w} (dh/dt)_{max}$$

but $mg \Delta h = \frac{1}{2} m (V_{max}^2 - V_{min}^2)$

so $$(dh/dt)_{max} = -\frac{W(V_{max}^2 - V_{min}^2)}{4g} \tag{57}$$

Substituting equations (39), (56), and (57) into equation (54) and assuming a wind shear of constant value k in the vicinity of the flight path;

$$Pa = \frac{-Wkw(V_{max}^2 - V_{min}^2) \sin wt \, (\overline{V} + \tfrac{1}{2} \Delta V \cos wt)}{4g^2} \tag{58}$$

The negative sign indicates that power is being supplied to the aircraft by the wind. The energy provided by

the climb is the same as that provided by the glide. Therefore the total energy supplied by the wind along the straight portions of the flight schedule is;

$$Ea = 2\left(-\int_0^{\pi/w} Pa\ dt \right)$$

$$Ea = \frac{4\ W\ k\ \overline{V}^2\ \frac{1}{2}\Delta V}{g^2} \tag{59}$$

In the level turns the wind will supply or extract energy from the aircraft. The power contribution of the wind is found from;

$$Pa = \frac{W}{g}\frac{dV_g}{dt}\ V$$

In the level turn

$$V_g = V + V_w \cos\Psi$$

$$V = \text{constant}$$

$$\frac{dV_g}{dt} = -V_w\ \sin\Psi\ \frac{d\Psi}{dt}$$

so $$Pa = -\frac{V\ V_w\ W\Omega \sin\Psi}{g} \tag{60}$$

For the turn at the high speed end (turning into the wind) the energy provided by the wind is;

$$Ea = -\int Pa\ dt = -\frac{1}{\Omega}\int_0^{\pi} Pa\ d\Psi$$

$$= -\frac{2\ V_{max}\ V_w\ W}{g} \tag{61}$$

Equation (61) shows that energy is extracted from the

aircraft in the high speed turn into the wind. For the turn at low speed away from the wind the integration shows that energy is supplied to the aircraft.

$$Ea = \frac{2\ V_{min}\ V_w\ W}{g} \tag{62}$$

Combining equations (61) and (62) yields the total energy contribution in the turns due to the wind;

$$Ea = \frac{2\ W\ \Delta V\ V_w}{g} \tag{63}$$

Thus the total energy available from the racetrack flight path is found by adding equations (59) and (63);

$$Ea = \frac{4\ W\ \Delta V}{2g}\left(\frac{\bar{V}^2}{g}\ k + V_w\right) \tag{64}$$

Comparing equation (64) with equation (38) shows that the racetrack flight schedule provides more energy from the wind by a factor of $4/\pi$.

EXPERIMENTAL RESULTS AND NUMERICAL ANALYSIS

Experimental investigation was conducted in a Beechcraft Bonanza Model F-33A airplane. This is a four seat low wing general aviation aircraft. It is powered by a Continental IO-520-BA reciprocating engine with rated maximum horsepower of 285 at sea level. The propeller is a constant speed two bladed type. All flights for data were made with gear and flaps retracted.

The aircraft was equipped with a drift sight located between the front and rear seats on the pilot's side. The drift sight was used to measure drift angles in straight and level flight. By triangulation methods wind speeds at flight altitudes were determined.

Figure 7 shows an upper level shear discovered on 24 March 1976. A non-linear shear interpretation has been indicated. The basis for this representation of the shear profile is the results indicated in Figure 3 of the Introduction. The presence of such a non-linear shear is also indicated by Figure 8.

Figure 8 depicts experimental results from glides in the area of the 24 March shear. The glides were made power off both with the wind and against the wind to verify the effect of wind shear predicted by equation (17). Altitude and elapsed time were recorded continuously throughout the

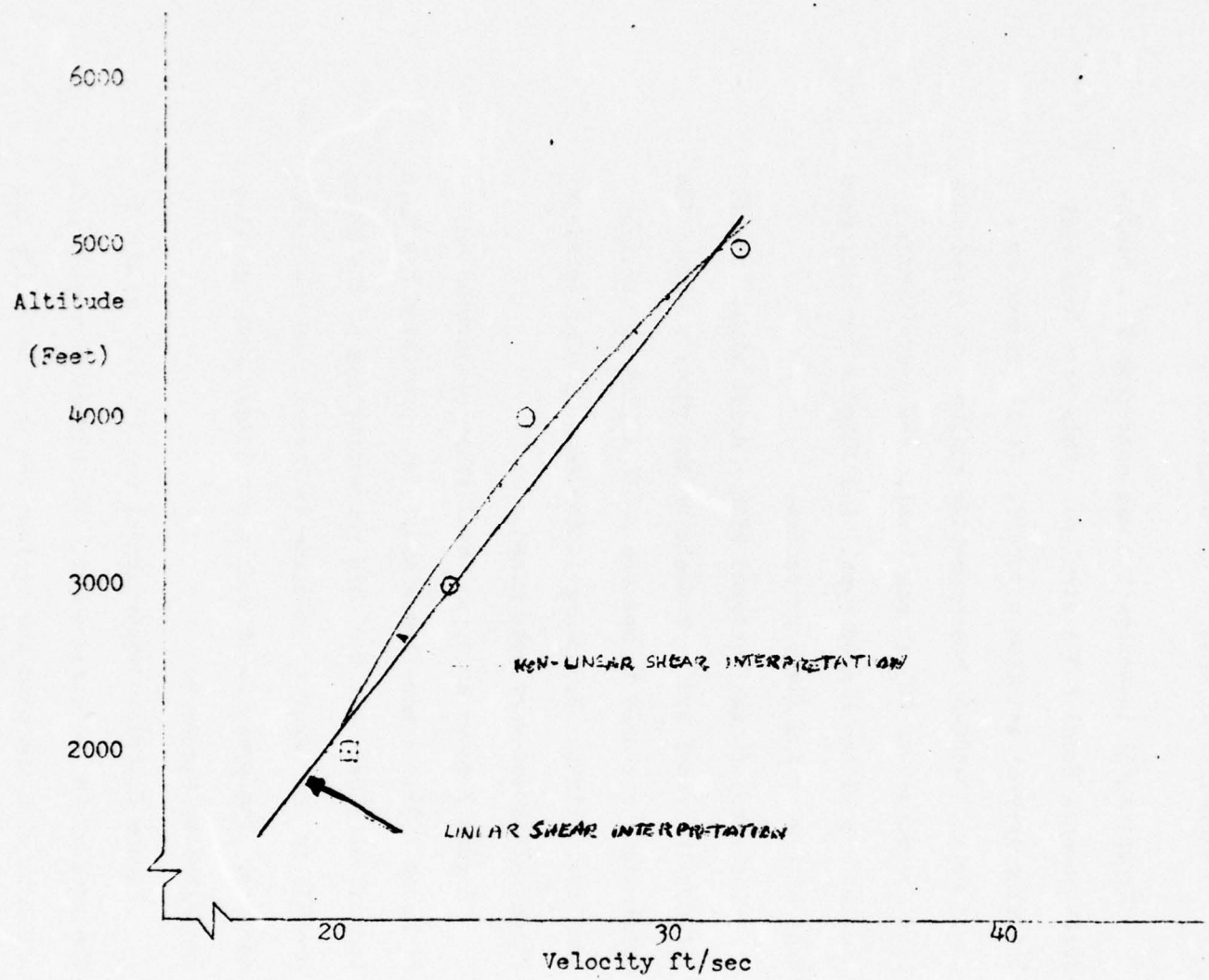

Figure 7. Upper level shear measured 24 March 1976.
Linear shear value .00389.

FIGURE 8. SINK RATE VERSUS SHEAR.

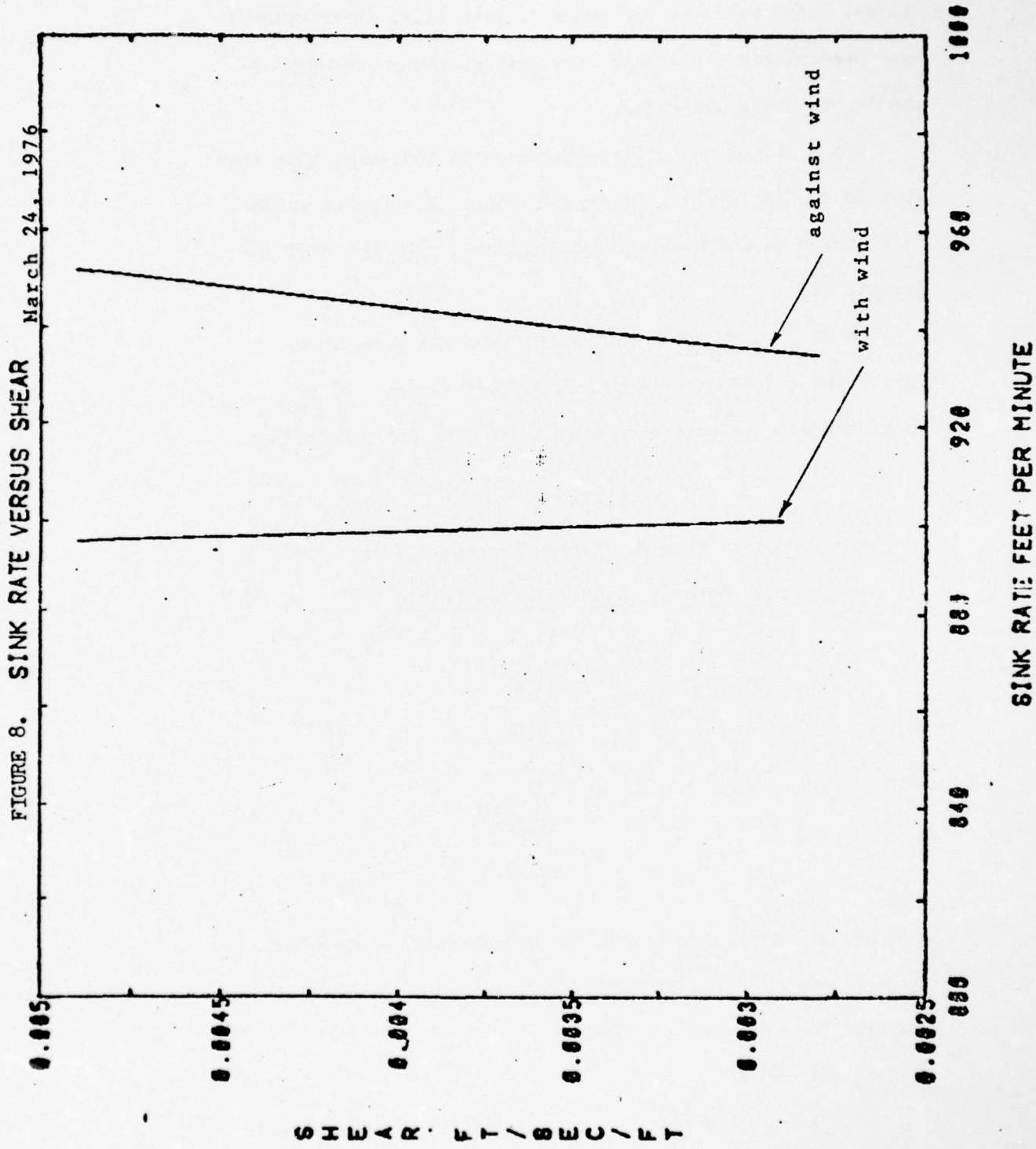

glides. Sink rates at various altitudes (i.e. shear values) have been plotted in linear form against the shears corresponding to those altitudes.

The plot for the glide with the wind indicates that sink rate is reduced with an increased shear. Also quite evident in Figure 8 is difference between gliding with the wind and against it.

On 14 January 1976 drift sight readings were taken to verify the existence of a boundary layer shear. Table 2 shows the wind velocities measured over the Chesapeake Bay.

Table 2

Boundary Layer Wind Velocities Measured 14 Jan. 1976

Altitude feet	Wind Velocity ft/sec
200	33
300	38.4
400	35.6
800	48.55
900	55.7
1000	64.53

The strength coefficient for Davenport's power equation was evaluated at each altitude and averaged to discover the equation for the boundary layer.

$$V_w = 16.68\ z^{1/7} \tag{65a}$$

$$dV_w/dz = 2.38\ z^{-6/7} \tag{65b}$$

Figure 9 is a plot of equation (65a) with data points indicated. Correlation is good and Davenport's power equation seems to adequately describe the boundary layer shear profile. Table 3 lists boundary layer wind parameters taken from equations (65a) and (65b).

Table 3

Wind Parameters In The Boundary Layer

Altitude feet	Wind Velocity ft/sec	Shear sec^{-1}
100	32.2	.046
200	35.6	.025
300	37.7	.018
400	39.3	.014
500	40.5	.012

Utilizing the boundary layer data obtained on 14 January for wind parameters, the Beechcraft Bonanza was evaluated for dynamic soaring performance using the racetrack flight technique.

A computer program was used to solve equations (53) and (64) for the aircraft flying in the region described by Table 3 (i.e. shears from approximately .01 to .08).

In addition, data from Appendix 1 was used; the airplane's performance at simulated superior glide ratios was investigated. Tables 4 and 5 indicate parameters used for the numerical analysis.

COMPARISON OF STANDARD BOUNDARY LAYER EQUATION TO RELIABLE DATA

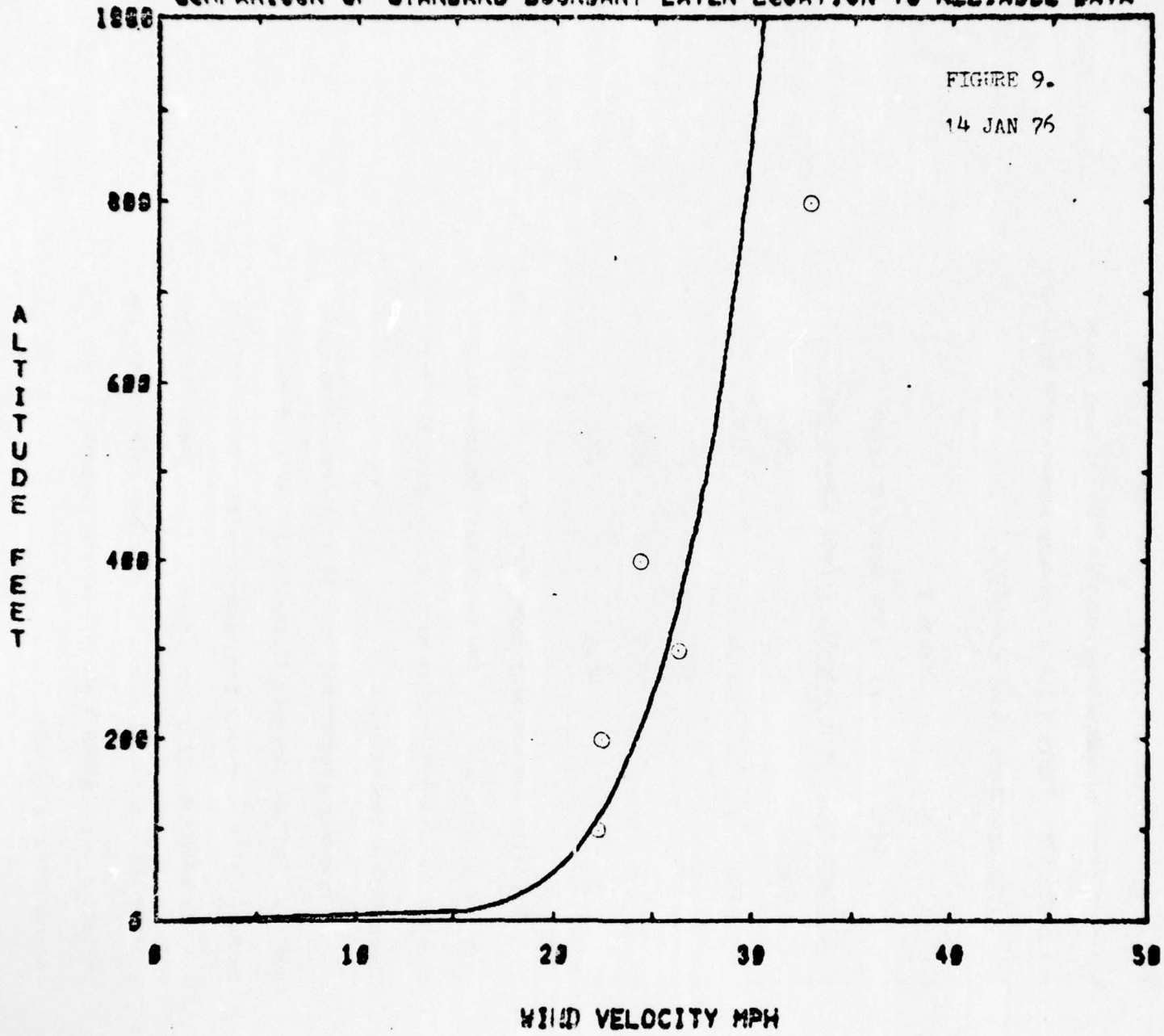

37a

Table 4	
Beechcraft Bonanza F-33A Performance Data	
Stall Speed, Power Off	74 MPH
Design Maneuvering Speed	152 MPH
Phugoid Period	23.7 seconds
V_{max}	152 MPH
V_{min}	88 MPH
$\overline{V}$	120 MPH
ΔV	32 MPH

Table 5

Beechcraft Bonanza F-33A Sink Rate Data

At Various Power Settings

(From Appendix 1)

Power Setting	R/S_o ft/s	V_o MPH
0%	14.3	88
15%	10	95
20%	8.8	98
25%	6.2	98
30%	4.6	99
35%	3.0	99
40%	1.5	101

Figure 10 is a plot of altitude gained (energy available divided by weight) in one racetrack cycle. The alti-

tude gained due to wind shear is independant of the sink rate performance of the aircraft but rather solely depends upon wind characteristics and velocity parameters chosen by the pilot.

Figure 11 shows the result of subtracting the altitude lost from the altitude gained for one racetrack cycle. As is clearly evident, at low power settings (low glide ratios) the net loss in altitude is totally unacceptable. Only with extremely high simulated glide ratios does the altitude lost begin to diminish to an acceptable value. Sailplanes with glide ratios of the order of magnitude necessary to produce a net increase in altitude per cycle do not exist today. Further numerical analysis of the dynamic soaring problem, utilizing actual sailplane parameters is warranted, however, in order to determine the true effect of the racetrack schedule upon high performance sailplanes.

FIGURE 10. ALTITUDE GAINED PER CYCLE DUE TO WIND.

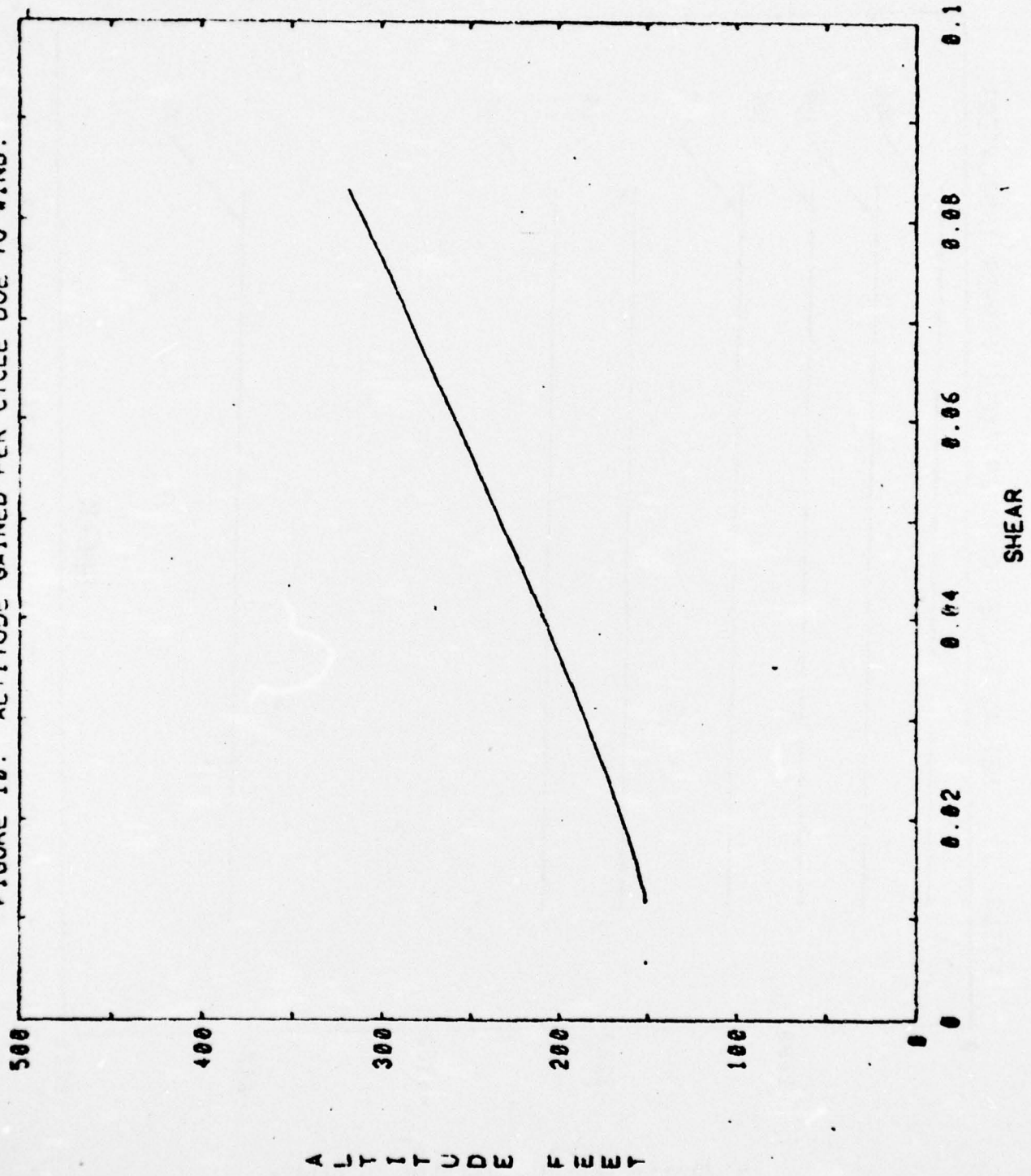

FIGURE 11. NET ALTITUDE LOSS PER CYCLE (POWER INDICATED).

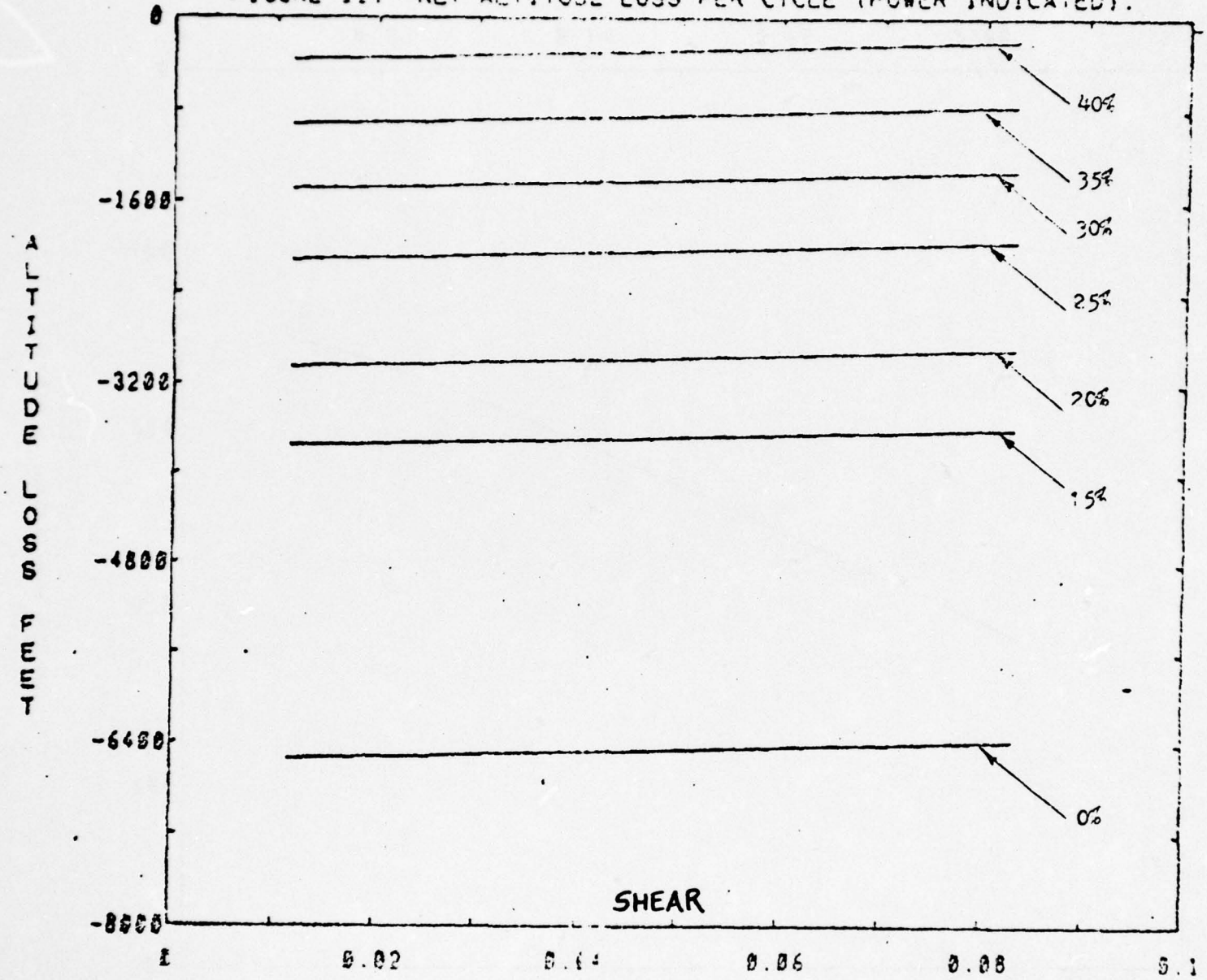

CONCLUSIONS

1. Wind shear may be used to increase the performance of an aircraft. This increase in performance may be expressed mathematically, and experimental observations concur with the theoretical predictions.

2. The wind shear found in the upper atmosphere (upper level shear) is not strong enough to provide the energy required to maintain continuous non-powered flight for even the best high performance aircraft. This does not rule out the possibility of a jet stream shear, however, which was not examined in this report.

3. Wind shear found in the lower part of the boundary layer is of the order of magnitude required to maintain continuous non-powered flight.

4. A racetrack flight pattern was found to be more condusive to practical application than the circular case from two standpoints. First, it turned out to be more efficient theoretically. Secondly it was much easier for the pilot to conform to the theoretical model for the racetrack than the circle.

5. The successful employment of the racetrack flight technique described in this paper greatly depends upon the aircraft's performance parameters. High glide ratio sailplanes would definitely be a requirement for achieving the objective of this study.

6. The numerical analysis of the racetrack flight schedule suggests a possible method for increasing the on station time of patrol aircraft operating in wind shear weather conditions. By properly employing wind shear at a reduced power setting a reduction in fuel consumption may be achieved.

7. The possibility of utilizing vertical wind currents (updrafts) in conjunction with horizontal wind shear was not explored by this paper. Such a topic is suggested as a basis for further investigation.

FOOTNOTES

[1] Hans Thomann, "Wind Effects On Buildings and Structures," American Scientist, 63 (1975), 278-287.

[2] James Luers and Jerry Reeves, "Effect of Shear on Aircraft Landing," CR-2287, July 1973, NASA.

[3] James Luers and Jerry Reeves, "Wind Shear Effects on the Landing of Aircraft," Journal of Aircraft, 12 (July 1975), 565-566.

[4] "NTSB Assays Iberia Accident at Logan," Aviation Week and Space Technology, 102 (7 April 1975), 54.

[5] A. G. Davenport, "Rationale For Determining Design Wind Velocities," Journal of the Structural Division, Proceedings of the American Society of Civil Engineers, 86 (May 1960), 43.

[6] Davenport, p. 48.

[7] U.S. Department of Commerce, National Oceanic and Atmospheric Administration, Summary Of Constant Pressure Data (WBAN 33), January 7, 1974.

[8] W. Bonner, "Climatology of the Low Level Jet", Monthly Weather Review, 96 (1968), 833-850.

[9] Dorathy Anne Stewart, "A Note On Wind Shear Near 80 W" Journal of Applied Meteorology, 6 (August 1967), 724.

LIST OF REFERENCES

Bonner, W. "Climatology of the Low Level Jet," Monthly Weather Review, 96 (1968), 833-850.

Davenport, A. G., "Rationale For Determining Design Wind Velocities," Journal of the Structural Division, Proceedings of the American Society of Civil Engineers, 86 (May 1960), 43.

Etkin, Bernard, Dynamics of Flight, New York: John Wiley & Sons, Inc., 1959.

Luers, James and Jerry Reeves, "Effect of Shear on Aircraft Landing," CR-2287, July 1973, NASA.

Luers, James and Jerry Reeves, "Wind Shear Effects on the Landing of Aircraft," Journal of Aircraft, 12 (July 1975), 565-566.

"NTSB Assays Iberia Accident at Logan," Aviation Week and Space Technology, 102 (7 April 1975), 54.

Soaring School Manual, Elmira , New York: Schweizer Aircraft Corp., 1971.

Stewart, Dorathy Anne, "A Note On Wind Shear Near 80°W," Journal of Applied Meteorology, 6 (August 1967), 724.

Thomann, Hans, "Wind Effects On Buildings and Structures," American Scientist, 63 (1975), 278-287.

U.S. Department of Commerce, National Oceanic and Atmospheric Administration, Summary of Constant Pressure Data (WBAN 33), January 7, 1974.

APPENDIX 1

SIMULATION OF SUPERIOR GLIDE RATIOS

Flight testing the concept of dynamic soaring in wind shear with a sailplane would require a great deal of time and expense. In addition, utilizing one sailplane limits the investigator to a single set of aircraft performance parameters. It is desirable to employ a single aircraft with variable sailplane characteristics which can make repeated test runs in a single flight. It is possible to do just that with a powered aircraft. Lift to drag ratios exceeding present sailplane maximums may be reached by applying a fraction of the power necessary to maintain level flight.

The aircraft to be used for experimental testing of dynamic soaring analytic results was the United States Naval Academy's Beechcraft Bonanza. A brief description of the process used to calibrate various aircraft power settings with glide ratios and results are contained herein. Actual intermediate curves and computer printouts are available from the author in a seperate unpublished report entitled "Simulation of Superior Lift To Drag Characteristics With A Powered Aircraft".

Power required and power available curves for the Beechcraft Bonanza were determined from actual inflight testing on October 9, 1975. Power required was ascertained from a linear plot of V^4 versus $P \cdot V$. Power available was

found from an acceleration run which produced excess power data. Excess power, when added to power required, produces the power available curve.

Percentage curves of the power available curve were then computed. These curves then became the zero line for power required and points from the former were subtracted from the latter. The result was a reduction in the effective power required and a resultant increase in glide ratio. Figure 6 displays effective power required curves (multiplied by 550 horsepower/ft-lb and divided by standard Beechcraft weight of 3400 pounds to yield sink rates) at power settings of various levels. Results of calculations are tabulated in Table 1.

TABLE 1.

Glide Ratios At Various Power Settings

Power Setting	L/Dmax
0%	11.57
15%	15.28
20%	18.89
25%	23.66
30%	31.27
35%	48.37
40%	96.73

FIGURE 6. SINK RATES AT VARIOUS POWER SETTINGS.

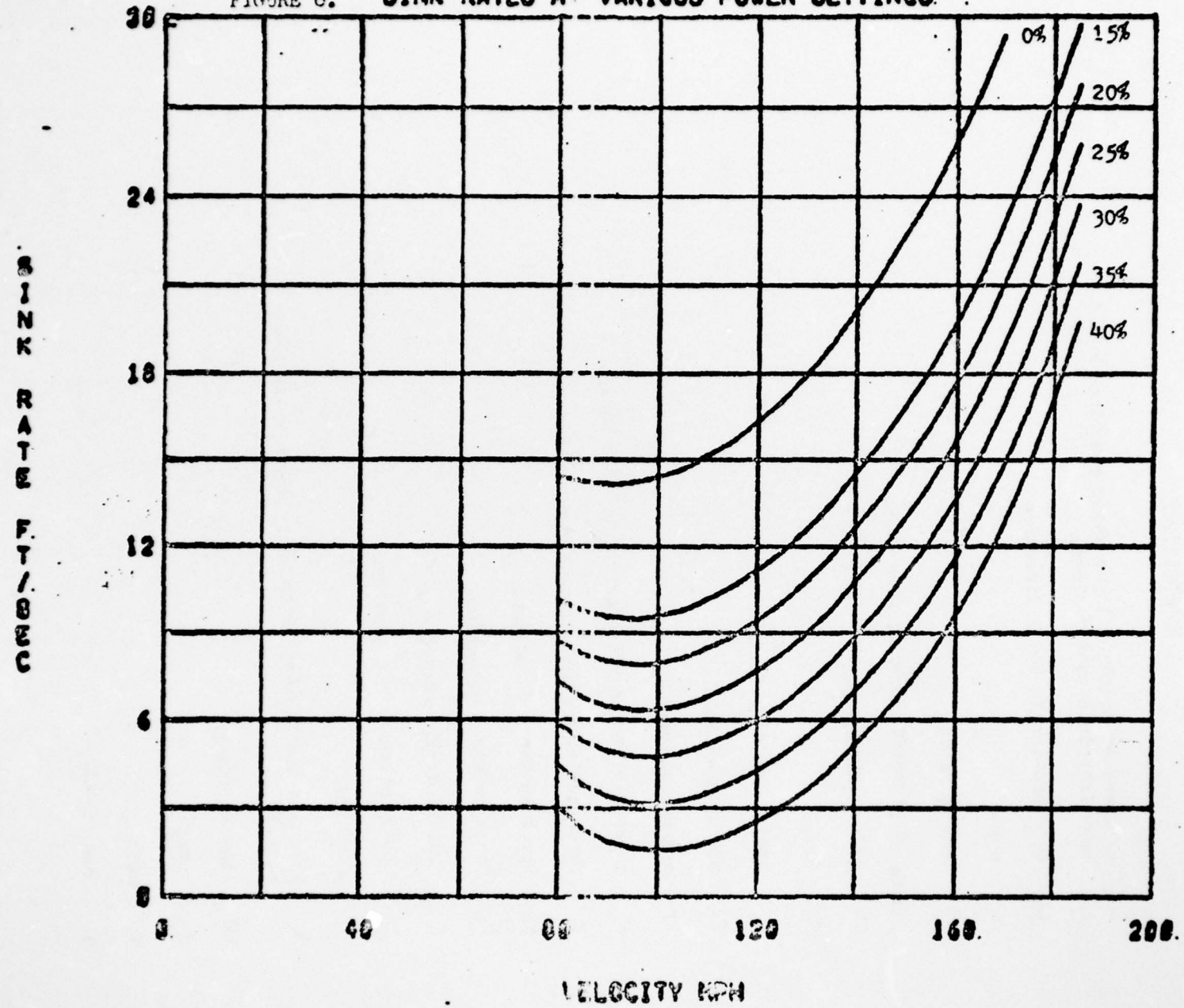

APPENDIX 2

NOMENCLATURE

a	exponent of boundary layer shear equation; based upon terrain considerations.
a_x	acceleration in the x direction.
A	$\pi AR\, e$
AR	aspect ratio.
C_{Dmin}	drag coefficient at zero lift.
C_L	lift coefficient.
D	drag.
e	span efficiency factor.
Ea	energy available.
Er	energy required.
F	descent efficiency factor due to wind shear.
F	force acting on the aircraft due to wind shear.
F_x	force in the x direction.
F_y	force in the y direction.
f	phugoid cyclic frequency.
g	acceleration due to gravity.
h	altitude.
k	strength coefficient of boundary layer shear power equation.
KE	kinetic energy.
L	lift.
m,M	mass.
n	load factor.

P power.

Pa power available.

Pr power required.

q dynamic pressure.

R/D rate of descent.

R/S_o minimum rate of sink.

S wing surface area.

t time.

V true airspeed.

Vg ground speed.

V_o speed for minimum sink rate (minimum power).

Vw wind speed.

Vy vertical velocity.

w phugoid angular frequency.

W weight.

z altitude.

γ flight angle.

Γ $\frac{1}{2}\rho S$

ρ density.

Ψ flight heading with respect to wind direction.

Ω angular rotation rate (turning rate).

Φ bank angle.

UNCLASSIFIED

Security Classification

DOCUMENT CONTROL DATA - R & D

(Security classification of title, body of abstract and indexing annotation must be entered when the overall report is classified)

1. ORIGINATING ACTIVITY (Corporate author) U.S. Naval Academy, Annapolis.	2a. REPORT SECURITY CLASSIFICATION UNCLASSIFIED 2b. GROUP

3. REPORT TITLE

Investigation into the feasibility of utilizing wind shear for obtaining continuous non-powered flight.

4. DESCRIPTIVE NOTES (Type of report and inclusive dates)

Research report.

5. AUTHOR(S) (First name, middle initial, last name)

Frederick G. Johnson.

6. REPORT DATE 3 June 1976.	7a. TOTAL NO. OF PAGES 50.	7b. NO. OF REFS 10
8a. CONTRACT OR GRANT NO. b. PROJECT NO. c. d.	9a. ORIGINATOR'S REPORT NUMBER(S) U.S. Naval Academy, Annapolis - Trident Scholar project report, no. 78 (1976) 9b. OTHER REPORT NO(S) (Any other numbers that may be assigned this report)	

10. DISTRIBUTION STATEMENT

This document has been approved for public release; its distribution is UNLIMITED.

11. SUPPLEMENTARY NOTES	12. SPONSORING MILITARY ACTIVITY U.S. Naval Academy, Annapolis.

13. ABSTRACT

The feasibility of utilizing an atmospheric velocity gradient for obtaining continuous non-powered flight was analyzed mathematically and experimentally.

It was discovered that there seems to be no theoretical bar to using wind shear for this purpose. The velocity gradients in the upper atmosphere were found to be too weak for maintaining continuous non-powered flight. But in the vicinity of the earth's boundary layer wind shear strengths necessary for this purpose were observed.

A theoretical flight pattern was developed - numerically analyzed and flight tested - using a powered aircraft to simulate high performance sailplanes. Though an increase in aircraft performance was realized, a zero net loss of altitude was not achieved.

It is concluded, however, that further research is warranted, especially concerning the related topics of jet stream shears, vertical updraft considerations and more efficient flight schedules.

DD FORM 1 NOV 65 1473 (PAGE 1)

S/N 0101-807-6801

UNCLASSIFIED.

Security Classification